JOURNAL OF PLANKTON RESEARCH | VOLUME 33 | NUMBER 6 | PAGES 947–959 | 2011

Environmental effects on phytoplankton production in a Northeast Atlantic fjord, Faroe Islands

EILIF GAARD [1]*, GUNNVØR Á NORÐI [1] AND KNUD SIMONSEN [2]

[1]FAROE MARINE RESEARCH INSTITUTE, TORSHAVN, FAROE ISLANDS AND [2]UNIVERSITY OF THE FAROE ISLANDS, TORSHAVN, FAROE ISLANDS

*CORRESPONDING AUTHOR: eilifg@hav.fo

Received July 7, 2010; resubmitted on November 3, 2010; accepted in principle November 12, 2010

Corresponding editor: William K. W. Li

Primary production in the fjords of the Faroe Islands is usually high. Results of productivity measurements in a typical Faroese fjord (Kaldbaksfjord) in 2006 and 2007 reveal values of about 335 g C m^{-2} $year^{-1}$, which is two to three times higher than reported from neighboring regions, such as Icelandic, west Norwegian and west Scottish fjords. The causal mechanism is high flushing rate of the euphotic zone and high influx of nutrients, relative to the surface area. On average, the majority of the production is based on new production. The productive season is from late March to early April until October. It is controlled by irradiance and occurs when the critical depth extends below the halocline. The system is highly dynamic and the plankton productivity is largely influenced by short-term fluctuations in horizontal flow and vertical mixing, influencing vertical as well as temporal variability in P/B ratio and f-ratio. Fast repetition rate fluorescence profiles revealed that F_v/F_m decreases below 0.5 when the light intensity is above 200 μE m^{-2} s^{-1} or when the nitrate + ammonium concentrations were below a threshold between 0.8 and 2 μM.

KEYWORDS: fjord; environment; primary production; FRR fluorescence

INTRODUCTION

In many estuarine systems, primary production is high (Mann, 2000). Freshwater runoff causes stratification, and due to nutrient influx and upwelling, induced by estuarine circulation, there is a continuous net nutrient transport upwards, into the euphotic layer. These effects (upwelling and stratification) create good conditions for phytoplankton growth.

Temperate estuarine systems furthermore are characterized by short-term fluctuations in hydrographic and chemical condition within the upper water layer, which are driven by, for example, wind, freshwater input and tides. In areas with a relatively shallow pycnocline and unstable weather conditions, such as in many high-latitudinal Atlantic fjords, the hydrographic properties affecting primary production are temporally highly variable. Wind strength and direction, precipitation, and tides may vary substantially within a short time, and affect the hydrographic conditions (mixing, upwelling, stratification and depth of the pycnocline). Such fjords can therefore often be considered as highly dynamic systems.

Periodically, increases and decreases in primary production may be triggered by alternating periods of stratification, mixing and changing nitrogen cycling (Fouilland *et al.*, 2007). This also affects the phytoplankton community structure in temperate estuarine systems, either directly through alternating periods of mixing and stratification (e.g. Margalef, 1978; Jones and Gowen, 1990) or indirectly through subsequent variability in nutrient concentrations and forms of nutrients (e.g. Egge and Aksnes, 1992; Rousseau *et al.*, 2002).

doi:10.1093/plankt/fbq156, available online at www.plankt.oxfordjournals.org. Advance Access publication December 14, 2010

Anthropogenic nutrient inputs may, in combination with natural features, such as nutrient mixing into the euphotic zone and stratification, ultimately result in increased phytoplankton growth. However, under circumstances with excess nutrients, anthropogenic nutrient load is expected to have a low effect on primary production. Conversely, when nutrients in the euphotic zone are depleted or limiting for phytoplankton growth, anthropogenic input might increase primary production.

Most fjords in the Faroe Islands are narrow (~1 km) and deep (30–60 m). Similar to many other estuaries, they are important nursery areas for a large number of fish stocks, including the commercially important cod and saithe (Steingrund *et al.*, 2005) and they are also extensively used in aquaculture and for other purposes.

Despite the intensive use of the fjords and their ecological importance for a large number of marine organisms, relatively little is known about basic features such as hydrographic conditions, primary production and processes in the pelagic environment. Such knowledge is essential in sustainable use of the fjord systems, as well as maintaining optimal water quality conditions and welfare for farmed fish.

In this study, the variable environmental influences on phytoplankton ecology, dynamics and processes in a typical Faroese fjord are investigated. The fjord is in many respects representative for several high-latitudinal northeastern Atlantic fjord systems. Due to its highly dynamic nature, high exchange rates and high productivity, the study reveals information on environmental effects on plankton dynamics in such fjord systems in general.

METHOD

Study area

The study was conducted in Kaldbaksfjord, Faroe Islands, located at 62°03N, 6°50W. The fjord is 6.6 km long and 0.5 to 1.7 km wide, with a surface area of 5.41 km^2 (Fig. 1), and the total volume is about 185 × 10^6 m^3. The maximum depth of the fjord is 60 m and at the entrance, there is a 40 m deep sill.

The fjord receives seawater from the Faroe Shelf and from a sound located just outside the fjord entrance. It furthermore receives fresh water from direct precipitation and through runoff from a ~42 km^2 catchment area in the surrounding mountains. Most of the catchment area is uncultivated and uninhabited, and thus the nutrient runoff from land is low compared with other nutrient sources. The main anthropogenic nutrient source is from fish farming activity in the fjord (Mortensen, 1990).

Due to its northerly location, the fjord receives a wide seasonal range in solar radiation, with day lengths ranging from 5 h in mid-winter to 20 h in mid-summer.

Sampling

Time series measurements were carried out at station T (Fig. 1). The bottom depth was 52 m. Samples were collected on 15 occasions, from March 2006 to May 2007, with higher sampling frequency during summer than during winter. All measurements were carried by day (between 10 a.m. and 2 p.m.). On each sampling date, salinity and temperature profiles were measured, and samples were collected at 1, 5, 10, 20 and 50 m for measurements of nutrients, chlorophyll *a* (Chl *a*) and particulate organic carbon (POC). Samples for phytoplankton species identification and enumeration were collected on selected dates at 1, 5, 10 and 20 m depth. Water for primary productivity measurements (^{14}C incubation) was collected at 5 and 20 m depth. Fast repetition rate fluorescence (FRRF) measurements were carried out in spring and summer 2007.

In addition to the time series, transect measurements of hydrography, Chl *a*, nutrients and primary productivity were carried out on two cruises (29 August

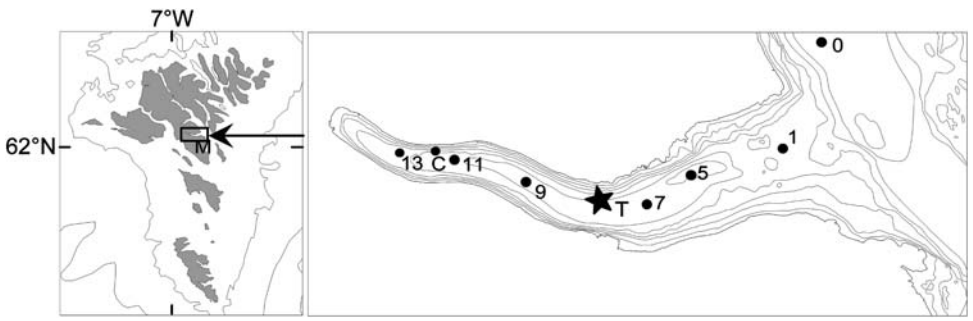

Fig. 1. Kaldbaksfjord and the meteorological station (M), centrally located on the Faroe Islands and location of the sampling stations.

2006 and 27 August 2007) with R/V Magnus Heinason (Fig. 1, stations 0–13).

Current profiles were measured from 6 m below the surface to the bottom at station C (38 m bottom depth) during the period 22 March–1 June 2006. Meteorological observations were obtained at a weather station in Torshavn, located about 5 km south of the fjord (Fig. 1, station M). The station is operated by the Danish Meteorological Institute. Altitudinal precipitation records were made by the local electrical power company.

Hydrography

For the time series, salinity and temperature profiles were obtained with a Seabird SBE 37-SM MicroCAT. The measuring frequency of the instrument was 5 s intervals per measurement. The instrument was lowered slowly by hand, obtaining two to three measurements per meter. The data were averaged to 1 m depth intervals by linear interpolation between measuring points. For the transects, temperature and salinity profiles were obtained using a Seabird 911plus CTD. These data were likewise averaged to 1 m depth intervals. Current velocity and direction were measured in 2 m bins using a RDI 300 kHz Work Horse bottom mounted Acoustic Doppler Current Profiler (ADCP).

Nutrients, POC, Chl *a* and phytoplankton

The nitrate and nitrite (hereafter nitrate) and ammonium samples were preserved with three droplets of chloroform per 20 mL of sample. Nitrate was measured on an autoanalyzer according to Grasshoff *et al.* (Grasshoff *et al.*, 1999), and ammonium was measured manually according to the salicylate-hyperchlorite method of Bower and Holm-Hansen (Bower and Holm-Hansen, 1980).

Chl *a* was measured spectrophotometrically according to Parsons *et al.* (Parsons *et al.*, 1984). Two liters of seawater were filtrated on Whatman GF/F filters, and the extraction was carried out with 90% acetone. The Chl *a* content was calculated using the equation of Jeffrey and Humphrey (Jeffrey and Humphrey, 1975).

Phytoplankton samples were preserved with Lugol solution. The algae were identified and counted using an inverted microscope after settlement overnight in 2 mL sample chambers. The cell sizes were measured and converted to carbon based on geometrical shapes and using a volume to carbon conversion factor of 0.13 for armored dinoflagellates and 0.11 for all other phytoplankton (Edler, 1979).

For measurements of POC content, 1 L of seawater was filtered through precombusted Whatman GF/F filters. In order to remove inorganic carbon, the filters were fumed with HCl prior to measurement on a CE 440 Elemental analyser.

Primary production

^{14}C incubations

Samples for production–irradiance (P–I) curves at 5 and 20 m depth, respectively, were transferred to 40 mL plastic bottles, and stored dark and cold until arrival at the laboratory 2–3 h later. After addition of 1.2 μCi of $H^{14}CO_3^-$, the bottles were immediately placed on a rotating wheel and incubated at *in situ* temperature $\pm 1^{\circ}C$ for 2 h. Philips TLD 15W/33 were used as the light source, giving 11 light intensities in the bottles, from 16 to 210 $\mu E\,m^{-2}\,s^{-1}$. In addition, two dark bottles from each depth were incubated. After incubation, the content of each bottle was filtered on Whatman GF/F filters, dried and stored in the dark until later analysis. Radioactivity was measured on a liquid scintillation counter (Packard Tri-Carb 1500) after addition of scintillation liquid. The dissolved inorganic carbon (DIC) content at 5 and 50 m depth was measured on an infrared gas analyzer (ADC-225-MK3) and an average DIC concentration of 25.5 g C m^{-3} was used for calculation of carbon assimilation rates.

The two photosynthesis–irradiance (P–I) curves (5 and 20 m depth) represent light adaptation of the phytoplankton from above and below the pycnocline, respectively. The Chl *a* normalized primary productivity at depth z was calculated according to Sakshaug *et al.* (Sakshaug *et al.*, 1992):

$$P_z^B = P_{max}^B \times \left(1 - e^{(-\alpha^B \times I_z / P_{max})}\right) \quad (1)$$

where P_{max}^B is the Chl *a* normalized light saturated primary productivity, α^B the photosynthetic efficiency and I_z the irradiance at depth z. No photoinhibition was observed at the light intensities that were used in the incubator (up to 210 $\mu E\,m^{-1}\,s^{-1}$). Daily primary production was calculated from the P–I curves, taking into account the *in situ* irradiance per hour and the Chl *a* content at 1, 5, 10, 20 and 50 m depth with linear interpolation between the measuring points.

Diel light intensity at depth was calculated from satellite observations averaged over the years 1996–2000 (www.satel-light.com), and depth profiles of the attenuation of photosynthetic active radiation (PAR). The calculated daily production represents the net production during the photosynthetic period, ignoring the dark respiration.

Fast repetition rate fluorescence

In situ phytoplankton photosynthetic parameters [equation (2)] were obtained using an FRRF (Chelsea Instruments,

Ser. No. 182061). The FRRF was equipped with a Chelsea Instruments spherical PAR sensor and a depth sensor. All profiles were taken facing toward the sun to avoid shading from the boat. The instrument was lowered gently to 50 m depth with a speed of 0.1–0.2 m s^{-1}, obtaining at least four measurements per meter.

The instrument was set to an acquisition sequence of 100 saturation flashes, 20 relaxation flashes and 10 ms sleep time between acquisitions. Primary productivity at depth was calculated using the equation of Smyth *et al.* (Smyth *et al.*, 2004):

$$P_{(\mathrm{FRRF})z} = 1.87 \times 10^{-4} \left(\frac{F_\mathrm{v}}{F_\mathrm{m}}\right)_z \sigma_{\mathrm{PSII}}(\mathrm{max}) I_z [\mathrm{Chl}a]_z \quad (2)$$

where $(F_\mathrm{v}/F_\mathrm{m})_z$ is the ratio between the variable fluorescence (F_v) and the maximum fluorescence (F_m) at depth z (in other words, the potential photochemical efficiency of the open PSII reaction centers at depth z, dimensionless), $\sigma_{\mathrm{PSII}}(\mathrm{max})$ is the maximum effective absorption cross-section of photosystem II measured when non-photochemical quenching is negligible (10^{-20} m^2 $photon^{-1}$), I_z (μE m^{-2} s^{-1}) is the irradiance at depth z and [Chl a]$_z$ is the Chl a concentration (mg m^{-3}) at depth z.

Water exchange rates

The average water exchange is estimated from Knudsen's relations (Knudsen, 1900):

$$V_\mathrm{in} = V_r \frac{S_\mathrm{out}}{S_\mathrm{in} - S_\mathrm{out}} \quad (3)$$

where V_{in} is the flux of in-flowing seawater, V_r the freshwater runoff and precipitation (m^3 s^{-1}), and S_in and S_out are the salinities of the (deep) in-flowing and the (shallow) out-flowing water, respectively.

Equation (3) is set up for an idealized two-layer system with an out-flowing surface layer above an inflowing lower layer. Often, a sharp pycnocline was not obvious and instead a wide transition depth range between these two layers was common (Figs 2 and 3). To estimate the average water exchange, a simplification was made that the mean salinity in the uppermost 10 m of the water column represents the out-flowing upper layer (S_out), and the mean salinity in the inflowing layer (S_in) is assumed to be the average salinity at 35–40 m depth (Table I).

Precipitation data were derived at 35 m altitude (Fig. 1, station M) while the highest mountains in the catchment area exceed 600 m. The average precipitation is significantly higher in mountain areas than at sea level. By including short time precipitation records at four different altitudes in the years 2000–2004, it is found that the mean freshwater forcing of Kaldbaksfjord is

$$V_\mathrm{r} = 1.47 P_\mathrm{r} A_\mathrm{catch} \quad (4)$$

where P_r is the precipitation in Torshavn and A_catch the precipitation catchment area. In the estimates, the applied P_r is the mean precipitation for a period of 13 days prior to the day of the actual measurement.

RESULTS

Transect overviews

Figure 2 illustrates two examples of environmental variables along a section through the fjord in summer. Both examples show typical estuarine circulation, separating the water column into an upper and a lower layer (Fig. 2). The nitrate concentrations were related to the water layers, with higher concentrations in the deeper layer. Primary production and Chl a content were likewise associated with the water layers, combined with the effect of nutrients and light conditions.

The two examples do, however, illustrate a dynamic system with spatial and temporal variability driven by local physical forces. On 28 August 2006 (Fig. 2, left panels), there was a light outward breeze (5 m s^{-1}) and the hydrographic parameters as well as nutrient concentrations showed an extensive upwelling in the innermost part of the fjord. The upwelling increased nutrient fluxes to the euphotic zone in the innermost part of the fjord, which resulted in increased primary production in the region. However, the effect from enhanced upwelling was only local. The other example (27 August 2007) (Fig. 2, right panels) represents calm weather with horizontally quite similar physical and chemical conditions for phytoplankton growth throughout the fjord. Although the transects show some degree of variability, the central fjord (station T; Fig. 1) generally represents the physical, chemical and plankton variables in the fjord.

Temporal hydrographical variability

The fjord is subject to highly variable weather conditions, with changing winds and precipitation within short time scales. Strong wind events with daily mean wind speeds of 15–20 m s^{-1} may happen all times of the year, although they are more frequent in winter. Seasonally, the precipitation was at its minimum in

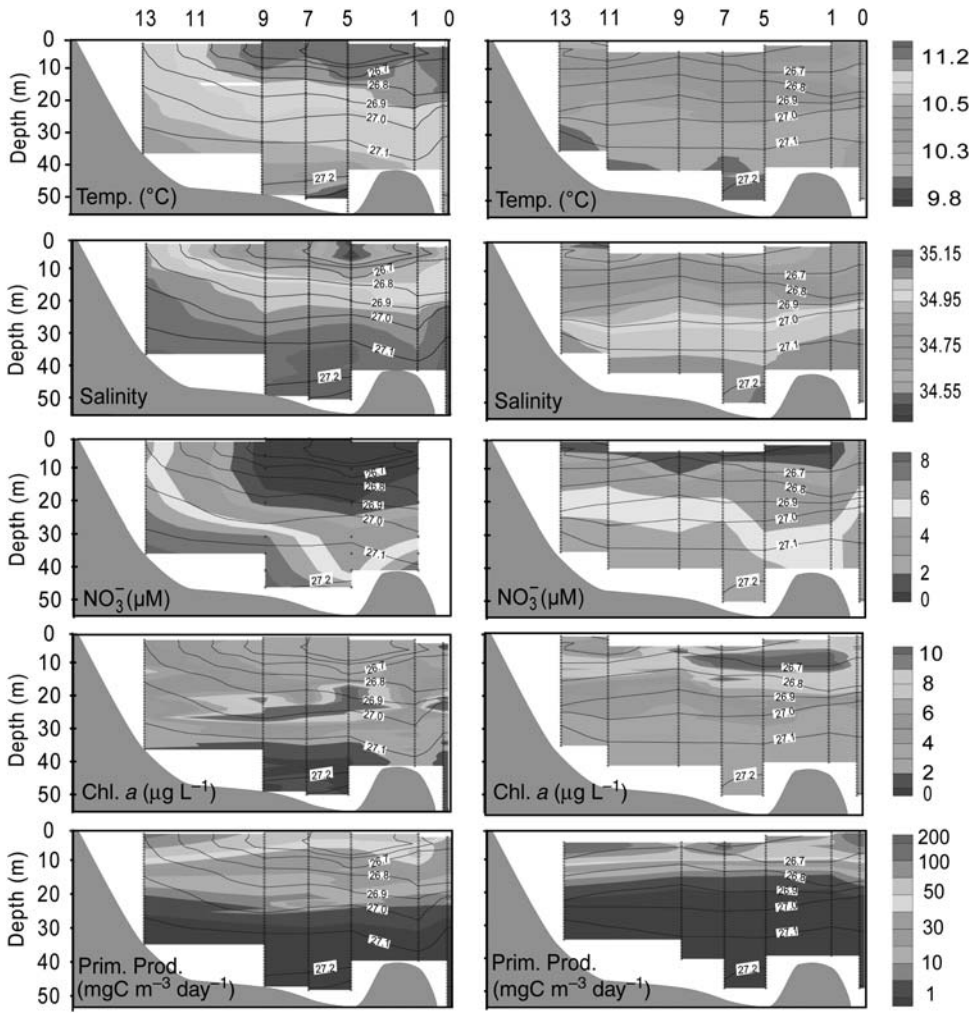

Fig. 2. Length sections of temperature, salinity, nitrate, Chl *a*, primary production and density (isopycnals in all panels) on 28 August 2006 (left panels) and 27 August 2007 (right panels). The numbers on the top refer to the sampling stations (Fig. 1).

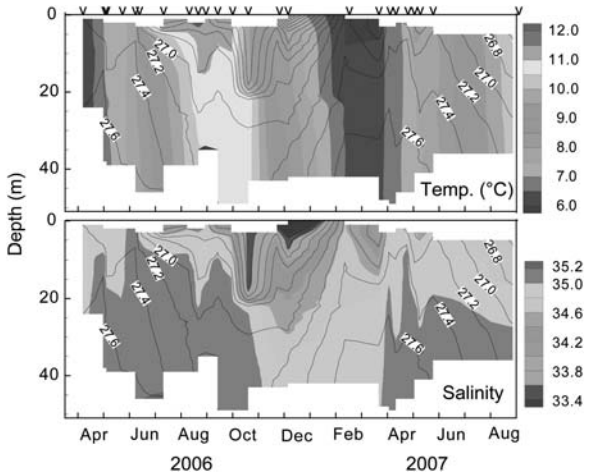

Fig. 3. Temperature, salinity and density (isopycnals on both panels) at station T between 22 March 2006 and 27 August 2007. V-marks indicate the sampling dates.

spring and summer 2006 and summer 2007 and maximum in autumn 2006 and winter 2007. One signature from the stronger wind mixing in winter, combined with relatively high monthly mean precipitation, is the enhanced mixing of fresh water into the water column (Fig. 3).

Vertical salinity depth gradients were observed year round. In the deeper layer, the salinity ranged between 35.0 and 35.2 in summer and between 34.6 and 35.0 in winter, while in the upper layer, it was more variable and usually ranged between 34.5 and 34.9 in summer and between 33.6 and 34.8 in winter (Fig. 3). Vertical temperature difference was usually small, and only in mid-late summer 2006 (June–September) did it exceed 2°C. Variations in density were mainly controlled by salinity, and only in summer did the temperature contribute slightly to the stratification (Fig. 3). The

Table I: Seasonal inflow and residence time of seawater in Kaldbaksfjord

Season	Dates	n	<S> 35–40 m	<S> 1–10 m	$<V_r>$ $m^3\ s^{-1}$	$<V_{in}>$ $m^3\ s^{-1}$	$<T_r>$ Days
Spring 06	05 May–08 June	4	35.12	35.00	1.51	448.5	4.8
Summer 06	08 June–29 Sept	7	35.15	34.79	1.57	152.0	14.1
Winter	13 Oct.–22 March	5	34.93	33.94	5.22	180.2	11.9
Spring 07	03 Apr.–25 May	6	35.09	34.81	1.89	236.2	9.1
Summer 07	27 Aug.	1	35.05	34.64	2.52	212.8	10.1

n is the number of measurement dates per season, *S* the mean salinity at station T, averaged for 35–40 and 1–10 m depth, V_r the mean seasonal freshwater runoff, V_{in} the estimated inflowing water to the fjord and T_r the residence time.

stratification was variable in depth and strength within short time scales.

Currents

The horizontal current velocity was usually low. At the location of the current measurements (the northern side of the fjord), the residual flow was in westward direction (inwards), with quite similar residual currents at all depths (Fig. 4). This implies that an eastward (outward) flow must exist in the southern side of the fjord, and this indicates effects from Coriolis forces on the water circulation. The average current speed was 3.5 cm s^{-1} and the strongest currents were in the 6–10 m depth range. Half of the time the speed was <4 cm s^{-1} and about 80% of the time, it was <6 cm s^{-1}. However, episodes did occur, with stronger currents and 1–2% of the time they were more than 14 cm s^{-1}. The variability in current velocity was highest in the upper layer. This most likely is due to wind effects.

The calculated exchange rates [based on salinity budget, equation (3)] ranged between 152 and 449 $m^3\ s^{-1}$. With a total volume of sea water in the fjord of 185×10^6 m^3, this corresponds to residence times between 5 and 14 days (Table I). The long-term average exchange rate was 234 $m^3\ s^{-1}$, equal to a mean residence time of about 10 days.

Nutrients

The winter concentrations of nitrate and ammonium were 11–12 and <0.2 μM, respectively, at all depths (Fig. 5). At the onset of primary production in spring, the nitrate concentrations in the upper layer decreased rapidly and were below 1 μM for a substantial part of the productive season, while in the deeper layer, most of the time they ranged between 5 and 8 μM. Events did, however, occur with increased concentrations in the upper layer during summer. The ammonium concentrations increased markedly in spring, and during summer they were on average clearly above the winter concentrations.

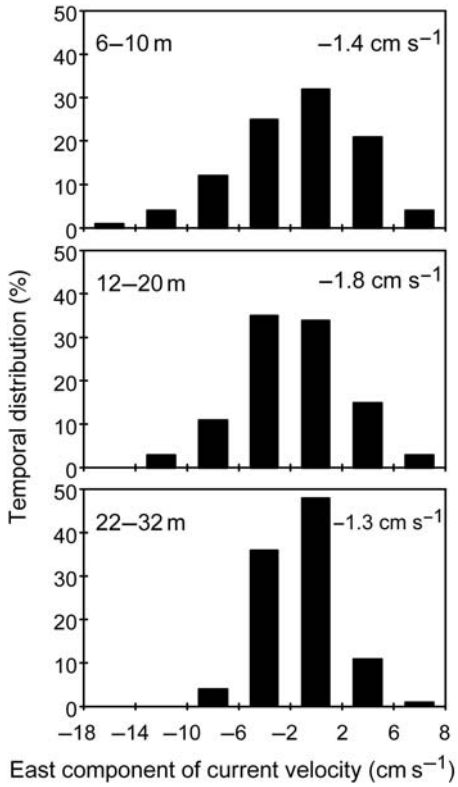

Fig. 4. The relative temporal distribution (in percent) of east component current velocities and the residual currents (figures) at station C, 22 March–1 June 2006 for three given depth intervals. Negative and positive current values represent westward and eastward direction, respectively.

Primary production and phytoplankton

The seasonal fluctuations in phytoplankton production and biomass were high, changing from very low levels in winter, to a highly productive system in spring and summer. During the productive season, the fjord was highly dynamic with large variability, temporally as well as vertically (Fig. 5).

The depth-integrated primary production fluctuated between 0.7 and 3.4 g C m^{-2} day^{-1} during the productive season (Fig. 6, upper panel). Seasonally, this high primary production reflected high Chl *a* values,

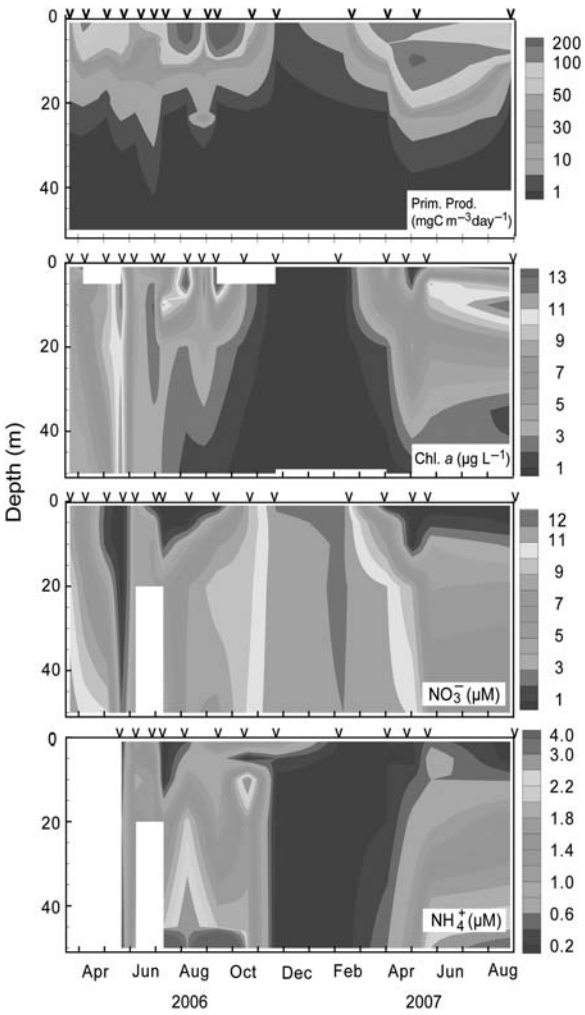

Fig. 5. Primary production, Chl *a*, nitrate and ammonium at station T between 22 March 2006 and 28 August 2007. V-marks indicate the sampling dates.

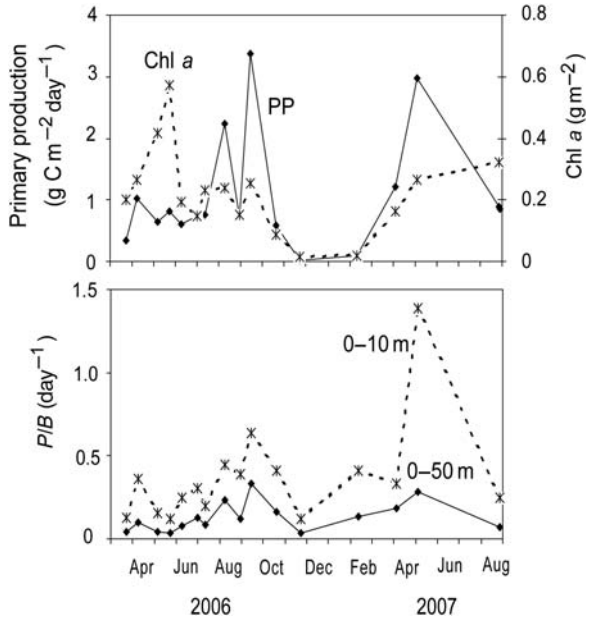

Fig. 6. Depth-integrated daily primary production and Chl *a* concentrations (upper panel) and specific primary production in the upper 10 and 50 m, respectively, at station T between 22 March 2006 and 28 August 2007.

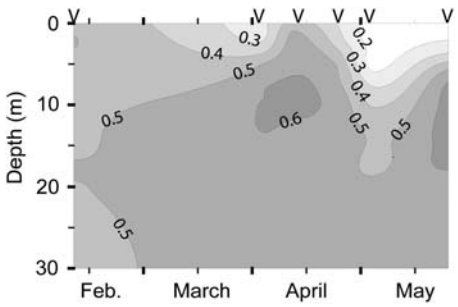

Fig. 7. F_v/F_m (at noon ± 2 h) in the upper 30 m at station T between 10 February and 25 May 2007.

which most of the productive season ranged between 200 and 400 mg m^{-2}. The annual primary production was about 335 g C m^{-2}, of which about 98% occurred between April and October.

There was a clear relationship between the Chl *a* concentrations and POC. A comparison between POC and Chl *a* concentrations at station T showed the relationship

$$\mathrm{POC} = 40.6\,\mathrm{Chl}\,a + 234.2 \quad (R^2 = 0.71,\ n = 45) \quad (5)$$

This conversion factor of 40.6 is used for calculating the *P/B* ratio, which is defined as the amount of assimilated carbon per day divided by the phytoplankton carbon biomass within the same water mass. The *P/B* ratio is thus a measure of daily phytoplankton growth per phytoplankton biomass (mg C mg C^{-1} day^{-1}). The temporally high fluctuations in *P/B* ratios (Fig. 6, lower panel) combined with the low relationship to total primary production strongly indicates that the short-term fluctuations in primary production were due to variable environmental conditions for phytoplankton growth rather than being driven by the phytoplankton standing stocks.

High vertical resolution in algal productivity, obtained by *in situ* measurements of active fluorescence (FRRF) from February to May 2007, showed variable maximum photochemical efficiency (F_v/F_m) with time and depth (Fig. 7). In winter, when irradiation was low and nutrient concentrations were high, the photochemical efficiency was close to maximum (~0.6) at all

depths. When experiencing stressful conditions, e.g. due to excess light or nutrient conditions, the efficiency rapidly decreases (Suggett *et al.*, 2009 and references therein). In spring and summer, photochemical efficiency in the upper 5–10 m was periodically low, and comparison of F_v/F_m profiles to simultaneously occurring light intensities and nutrient concentrations showed a combined dependency of F_v/F_m on light and nutrients. At light intensities above 200 μE m^{-2} s^{-1}, F_v/F_m was always below 0.5, regardless of high nutrient concentrations. Due to fewer nutrient measurements than light measurements, the threshold for a nutrient effect on quenching is more uncertain. F_v/F_m was reduced below 0.5 when the nitrate + ammonium concentrations were below a threshold between 0.8 and 2 μM. Thus, some light-induced quenching indeed may occur in the upper few meters around noon during summer.

Despite the temporal fluctuations in primary production, the short-term variability in phytoplankton species composition was small. However, between seasons and years, large changes were observed. In spring and summer 2006, large-sized diatoms of the genus *Coscinodiscus* sp. (diameter ~120 μm) completely dominated the phytoplankton biomass (Fig. 8). Although smaller sized diatoms (mainly *Leptocylindrus minimus*, *Pseudo-nitzschia longissima* and *P. delicatissima*) and various small-sized flagellates occurred in higher numbers than *Coscinodiscus* sp., they contributed little to the phytoplankton biomass compared with the much larger *Coscinodiscus* cells. In late summer, the community changed to dominance by small flagellates.

The spring and early summer season 2007 showed quite different species composition than the previous year, with medium- and small-sized algae dominating the phytoplankton community (Fig. 8). These were mainly small flagellates, and diatoms belonging to the genera *Leptocylindrus*, *Thalassiosira*, *Chaetoceros* and *Rhizosolenia*.

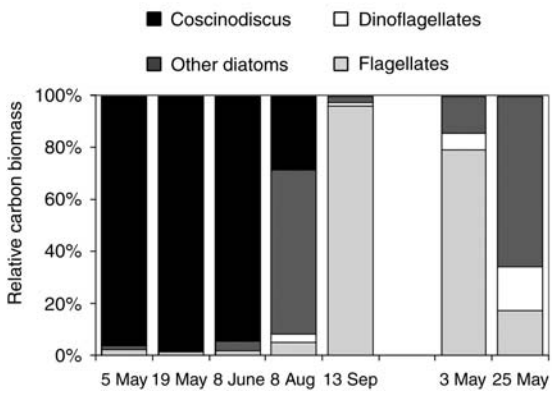

Fig. 8. Relative biomass contribution of phytoplankton groups in the upper 20 m at station T between 5 May 2006 and 25 May 2007.

DISCUSSION

The annual primary production estimate of 335 g C m^{-2} is consistent with a highly productive system. The value is markedly higher than in other fjords adjacent to the northern Northeast Atlantic. In Iceland, values around 120–180 g C m^{-2} $year^{-1}$ have been reported (Thordardottir 1976; Gudmundsson 2002), west of Scotland, they are around 140 g C m^{-2} $year^{-1}$ (Rees *et al.*, 1995) and in Norwegian fjords, typical annual primary production rates are 110–140 g C m^{-2} $year^{-1}$ (Eilertsen and Taasen, 1984; Erga, 1989). The reason for this high Faroese production is high exchange rate of sea water and inflow of nutrients from outside the fjord, relative to the fjord surface area, as discussed below.

Hydrography

The low salinity difference between the upper and lower layer causes a strong estuarine-driven circulation in the fjord. Due to the observed short-term temporary variable precipitation and salinity content in the upper layer, equation (3) cannot provide reliable exchange rate estimates on short time scales. However, on long time scales (months or more), the salinity balance is expected to provide fairly good average exchange rate estimates. Knudsen's relation assumes that all freshwater is equally distributed over the surface area. However, Fig. 4 indicates a Coriolis effect in the fjord, forcing the water toward the right and causing a weak anti-clockwise horizontal circulation, in addition to the estuarine circulation pattern. A fraction of freshwater from the southern side of the fjord may, thus, leave along the southern coast, instead of being equally dispersed over the surface, causing a potential minor overestimation of the exchange rates. This may partly be counteracted by the chosen simplification by excluding the transition zone between the upper and lower layer in the application of the Knudsen relation [Equation (3)], which in general causes an overestimation of the salinity difference, and thus an underestimation of the exchange rates.

Seasonal variability in primary production

Due to the light-dependent effect on the algal photosynthesis/respiration ratio, the spring bloom cannot commence before the critical depth is greater than the

depth of the upper mixed layer (Sverdrup, 1953). Nelson and Smith (Nelson and Smith, 1991) presented a reformulation of Sverdrup's equation to

$$D_{cr} = \frac{\Sigma I_o}{(3.78 K_d)} \quad (6)$$

where D_{cr} is the critical depth (m), ΣI_o the time-integrated incoming PAR for a 24 h period (E m^{-2} day^{-1}) and K_d the light attenuation coefficient (m^{-1}). The length of the productive season is thus controlled by the daily irradiance (i.e. irradiation intensities and day lengths) combined with depth of the upper mixed layer.

The water column was stratified at all seasons, with highest density differences during winter (Fig. 3). However, due to the northerly location, the seasonal differences in daily irradiance are large. During winter (November–February), the critical depth was within the upper 1–3 m and practically no density difference was observed above this shallow depth range (Fig. 9, upper panel). Increased daily irradiance during spring caused the critical depth to reach below density gradients in March–April, and at the same time, the apparent primary production increased. Thus, the productive season seems to have been controlled by seasonal changes in critical depth (due to changes in day lengths and surface irradiation) rather than changes in stratification.

The depth integrated *P/B* ratio was in the range of ~0.1–0.3 mg C mg C^{-1} day^{-1} (Fig. 6, lower panel)

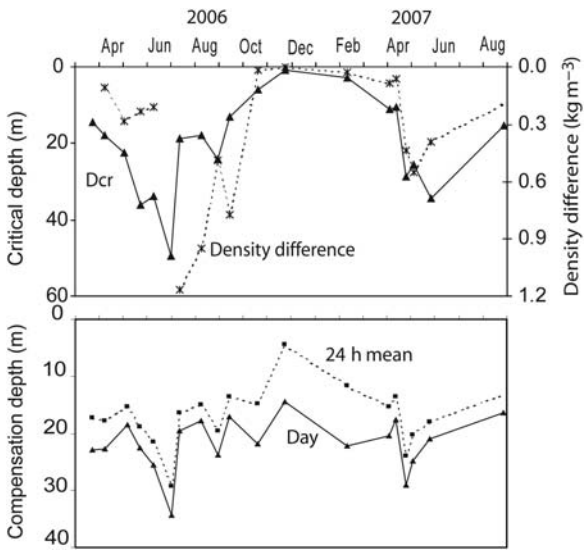

Fig. 9. Upper panel: Critical depth and density difference between 1 m depth and the critical depth at station T, between 22 March 2006 and 28 August 2007. Lower panel: Compensation depth at daylight (mean at noon ±2 h) and 24 h mean.

which implies a long-term mean renewal time of the phytoplankton standing stock of about 3–6 days. On average, this is less than the estimated mean renewal time of seawater (~10 days, Table I). The phytoplankton community within the fjord can therefore, be considered as mainly locally produced, although algal advection in periods certainly influences the standing stock.

Despite the temporal fluctuations in primary production, short-term variability in phytoplankton species composition was small. However, between seasons and years, large changes were observed. In spring and early summer 2006, the very large diatom *Coscinodiscus* sp. dominated the biomass and in mid-summer 2006, the phytoplankton community changed to dominance of small-sized diatoms and flagellates. In 2007, *Coscinodiscus* sp. was absent and instead flagellates and small diatoms dominated. Larger diatoms might, however, have been abundant during short periods in early spring without being observed in our measurements.

Several environmental circumstances are needed for such large *Coscinodiscus* cells to dominate: Under non-limiting nutrient conditions, diatoms in general have faster growth rates than smaller flagellates (e.g. Langdon, 1988). However, at low nutrient concentrations, small cells may have a competitive advantage, due to their larger surface area per cell volume than large cells (Kiørboe, 1993). Secondly, large cells tend to sink substantially faster than small cells, unless vertical water movements support their suspension in the water column (Mann and Lazier, 2006). During the spring and early summer 2006, when *Coscinodiscus* was abundant, the vertical mixing seemingly was especially strong (Table I, Fig. 5).

After the spring bloom in May, the primary production in the surface layer was to a large extent controlled by nutrient limitation. During the productive season, the mean nitrate concentrations 50–60% of the time were ≤1.5 μM in the upper 10 m and ≤1.0 μM in the upper 2 m of the water column. This nutrient depleted period is, however, considerably less than in comparative areas, such as Norwegian fjords (e.g. Erga, 1989; Aure *et al.*, 2007) and Scottish lochs (Rees *et al.*, 1995). The difference is most likely due to frequently occurring events with high vertical mixing in this system, as verified in the time series measurements of hydrographic conditions. At periods with increased vertical mixing and upwelling, the nutrient concentrations in the upper layer increase, and shortly after such events, the conditions for primary production in the upper layer become very good. However, provided that strong mixing events do not increase the estuarine circulation substantially, such events are expected to decrease

the total annual production, since excess (un-assimilated) nutrients then are exported in the upper layer during the mixing events.

Vertical variability in primary production

The compensation light intensity may vary between algal species and light adaptation. Marra (Marra, 2004) suggested it to vary between 1.2 and 3.5 $\mu E\,m^{-2}\,s^{-1}$ while others have suggested it to be slightly higher at about 4 $\mu E\,m^{-2}\,s^{-1}$ (K. Gudmundsson, pers. comm.). Assuming an average compensation light intensity of 3 $\mu E\,m^{-2}\,s^{-1}$, the compensation depth during daylight was mostly around 20 m (Fig. 9, lower panel). It was fairly constant most of the year, and only occasionally (during low Chl *a* events in summer) did it exceed 25 m. The euphotic zone, thus, covered the entire upper layer (assumed to be 10 m deep) and the uppermost part of the lower layer, during the productive season.

Earlier studies have indicated that nitrogen rather than phosphate is usually the limiting nutrient in Faroese fjords (unpublished data). Despite frequent periods with low nitrate concentrations in the upper layer, 73% (±12% st. dev.) of the annual production occurred in the top 10 m (Table II). The fraction fluctuated between 49% and 95% and no seasonal trend could be observed. However, the production in the upper 1–3 m may have been slightly overestimated in summer, since the light intensities used in the incubation experiments did not suggest that potential photoinhibition be included in calculations of the primary production [Equation (1)].

On average, the FRRF technique gave 1.8 (±0.2 SE) times higher production estimates than the ^{14}C incubation technique. This is slightly higher than the 1.5 factor found by Debes *et al.* (Debes *et al.*, 2008) using the same instrument on the Faroe shelf. There are several potential causes for primary production estimates by the FRRF technique to be higher than those obtained by the ^{14}C technique (Debes *et al.*, 2008). The most important is that the FRRF technique measures gross electron transfer rate while the ^{14}C technique can be assumed to approximate net production in incubations of 2–4 h (Jespersen, 1994; Marra, 2002). Since there are different sources of potential errors associated with these two different techniques, it is difficult to compare the two sets of results (Debes *et al.*, 2008), and the 1.8 factor does not necessarily provide exact information on the net versus gross productivity. However, the FRRF technique seems to be a reliable approach to obtain high vertical resolution measurements and their relation to environmental conditions (e.g. stratification, nutrients and light) in the field.

High resolution in vertical dynamics in phytoplankton growth conditions is exemplified in Fig. 10. When stratification is strong and nutrients are depleted in the upper layer, the phytoplankton biomass and production peak is located in the transition zone between the two layers, i.e. close to the nutricline (Fig. 10, left panels). The subsurface peak apparently was to a large extent

Table II: Seasonal mean depth integrated primary production (g C m^{-2} day^{-1}) in the upper layer (top 10 m) and below 10 m depth at station T

Season	Dates	*n*	1–10 m	11+ m	Total euphotic layer
Spring 06	May–June	3	0.52	0.21	0.73
Summer 06	June–Sept.	6	1.09	0.21	1.30
Winter 06/07	Oct.–Feb.	3	0.10	0.03	0.13
Spring 07	Apr.–May	2	1.25	0.84	2.09
Annual mean			0.74	0.18	0.92

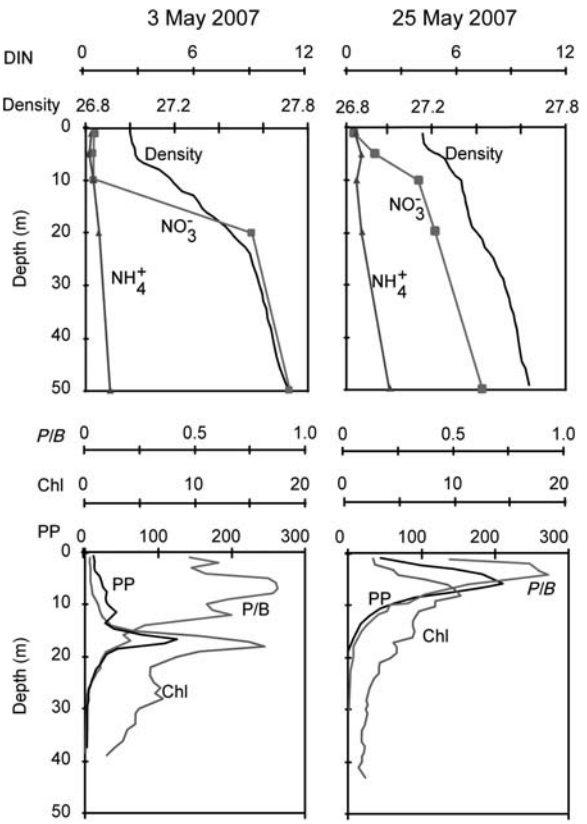

Fig. 10. Vertical profiles of density, nitrate and ammonium concentrations (upper panels) and FRRF measured primary production, Chl *a* and production/biomass (lower panels) at station T on 3 May and 25 May 2007.

fueled by new nutrients during their upward flux. However, the weight-specific growth rates (*P/B* ratios) were substantially higher in the upper layer than further down. Since the nutrient concentrations were low in the upper layer, this high productivity per unit biomass was apparently fueled largely by regenerated nutrients with high turnover rates.

Following events with increased vertical mixing (Fig. 3), measurements 3 weeks later showed that the nutricline had moved upwards and the subsurface peak in Chl *a* and primary production was located closer to the surface as well (Fig. 10, right panels). In this situation, a higher fraction of the primary production in the upper layer apparently was fueled by new nutrients, since the nitrate concentrations in the upper layer were substantially higher than in the situation 3 weeks earlier. Thus, due to temporally variable mixing events (largely induced by wind) the *f*-ratio in the upper layer is most likely highly variable with time, reflecting the temporally variable nutrient concentrations in this layer.

Figure 10 furthermore illustrates that the phytoplankton biomass peak may be located several meters below the depth of the highest productivity per unit biomass. The mechanism behind this may be a combined effect of phytoplankton sinking, increasing seawater density with depth, and reduced light intensities with depth. While sinking, the algae reach slightly denser water, which reduces their sinking speed. In the meantime, they experience lower light intensities, resulting in lower specific photosynthetic activity. At, for example, 10 m depth, the light intensity during daylight was typically around 30–60 $\mu E\ m^{-2}\ s^{-1}$, which is close to the half-saturated light intensities. Thus, while 'sitting' on the pycnocline, they still are able to obtain some photosynthetic activity under high nutrient concentrations. The subsurface photosynthetic maximum per volume is thus a result of high phytoplankton biomass, growing on upwelling nutrients while algae situated higher in the water column, on the other hand, experience higher light intensities and high turnover rates.

Nutrients supporting the primary production

A prerequisite for the very high primary production is a correspondingly high nutrient input into the euphotic zone (the top ~20 m). These nutrients may originate from below the euphotic zone, through precipitation or from anthropogenic sources (new production) or they may be regenerated nutrients, originating from heterotrophic recycling of organic matter within the euphotic zone (regenerated production) (Dugdale and Goering, 1967). Assuming that the primary production estimates at station T were representative for the fjord, the mean production (May–September) was about 1.5 g C $m^{-2}\ day^{-1}$. Using the Redfield ratio, this corresponds to a mean daily nitrogen demand of 0.27 g N $m^{-2}\ day^{-1}$.

Estimates of nutrient input into the euphotic zone in the fjord can be made based on calculated flushing rates (Table I), and nutrient concentrations in the water entering the euphotic layer from below (Fig. 5) and adding the nutrient load from precipitation and anthropogenic sources. Long-term averaged flushing rates are estimated to be in the range of 230 $m^3\ s^{-1}$ (Table I), corresponding to a net upwelling of about 4.5 m day^{-1}, giving an upwelling of nitrate and ammonium at 20 m depth (entering the euphotic zone) between May and September 2006 of 0.38 g N $m^{-2}\ day^{-1}$. This nitrogen comprises an inflow through the deep layer in addition to smaller amounts that are released from the sediment (á Norði, unpublished data). In addition, there was an input of anthropogenic dissolved inorganic nitrogen (DIN), directly into the euphotic layer. This is estimated to be 0.03 g N $m^{-2}\ day^{-1}$, of which the vast majority was from fish farming (assuming that 36% of the nitrogen in feed is excreted from the fish directly into the euphotic layer. (Bergheim and Aasgaard, 1996) while smaller amounts are from precipitation and runoff from land (Mortensen, 1990). The total mean DIN input to the euphotic zone thus was about 0.41 g N $m^{-2}\ day^{-1}$. The mean nitrogen demand of primary production during the same period was 0.27 g N $m^{-2}\ day^{-1}$ and thus the average amount of DIN input was more than adequate to support the high primary production, even with uncertainties in exchange rates of seawater taken into account.

As pointed out earlier, periodically high nutrient concentrations occurred in the upper 10 m, and assuming a net out-flush of these nutrients through the upper layer of 230 $m^3\ s^{-1}$, the mean loss of un-assimilated dissolved inorganic nutrients (mainly nitrate) through export in this layer can be estimated to about 0.21 g N $m^{-2}\ day^{-1}$. Thus, the average net uptake of new nutrients in the euphotic zone has been in the range of 0.20 g N $m^{-2}\ day^{-1}$ which is in the size range of 70–75% of the above-mentioned nitrogen demand of 0.27 g N $m^{-2}\ day^{-1}$. These values seem reasonable, since other nitrogen processes are involved in primary production as well. Most important is recycling of nitrogen, and in addition an unknown value of microbial uptake.

In productive areas, the fraction of new production relative to the total production (the *f*-ratio) is often around 0.5 and in upwelling systems, such as estuaries, it is expected to be even higher. In a Scottish sea loch, Rees *et al.* (Rees *et al.*, 1995) found, based on incubation

experiments of ^{15}N combined with ^{14}C incubations, that ~57% of the annual production was supported by nitrate uptake. Similar results are found in a number of other North Atlantic temperate fjords (Wassmann, 1990).

There are no direct estimates of new versus regenerated primary production in the present study. However, the estimate presented above implies that the fraction of potential new production, as defined as production based on nitrogen imported to the euphotic zone, on average possibly was in the range of 70–75% of the total primary production. There are indeed large uncertainties in such indirect estimates, and the value is indicative only. The estimate is sensitive to the seawater exchange rate estimates, which is discussed earlier and also short-term variability in vertical nutrient mixing (Figs 5 and 10). The exchange estimates should thus be considered as approximate long-term values.

The high primary production in this system is mainly a consequence of high flushing rates and of high upwelling, relative to the surface area. These values are clearly higher than commonly reported for other temperate Northeast European fjords (e.g. Arneborg, 2004; Gillibrand *et al.*, 2005).

The amount of imported nutrients from outside the fjord depends on the nutrient concentrations on the Faroe shelf during spring and summer. These are also highly variable from one year to another, with nitrate concentration during summer (May–September) ranging between 2.2 and 10.2 μM (Hansen *et al.*, 2005; Gaard *et al.*, 2006; Debes *et al.*, 2008). In 2006, the nutrient concentrations were above average and in 2007, they were close to the long-term average. Thus, the potential for annual new production in such fjords is also variable, depending on the available nutrient concentrations in the shelf water.

ACKNOWLEDGEMENTS

We want to thank the fish farming company P/F Týggjará for assistance in the field and the local electricity company SEV and the Danish Meteorological Institute for providing precipitation records.

FUNDING

Thanks to Statoil Faroes, Cheveron, The Faroese Research Council, the Aquaculture Research Station of the Faroes, and Geysir Petroleum for funding of the research.

REFERENCES

Arneborg, L. (2004) Turnover times for the water above sill level in Gullmar Fjord. *Cont. Shelf Res.*, **24**, 443–460.

Aure, J., Strand, Ø., Erga, S. R. *et al.* (2007) Primary production enhancement by artificial upwelling in a western Norwegian fjord. *Mar. Ecol. Prog. Ser.*, **352**, 39–52.

Bergheim, A. and Aasgaard (1996) Waste production from aquaculture. In Baird D. J., Beveridge, M. C. M., Kelly, L. A. and Muir, J. F. (eds), *Aquaculture and Water Resource Management*, Blackwell Science, Oxford, UK. pp. 50–80.

Bower, C. E. and Holm-Hansen, T. (1980) A salicylate-hypochlorite method for determining ammonia in seawater. *Can. J. Fish. Aquat. Sci.*, **37**, 794–98.

Debes, H., Gaard, E. and Hansen, B. (2008) Primary production on the Faroe shelf: temporal variability and environmental influences. *J. Mar. Syst.*, **74**, 686–697.

Dugdale, R. C. and Goering, J. J. (1967) Uptake of new and regenerated forms of nitrogen in primary productivity. *Limnol. Oceanogr.*, **12**, 196–206.

Edler, L. (ed.) (1979). *Recommendation on Methods for Marine Biological Studies in the Baltic Sea. Phytoplankton and Chlorophyll*. The Baltic Mar. Biol. Publ., Vol. 5, pp. 1–38.

Egge, J. K. and Aksnes, D. L. (1992) Silicate as regulating nutrient in phytoplankton competition. *Mar. Ecol. Prog Ser.*, **83**, 281–289.

Eilertsen, H. C. and Taasen, J. P. (1984) Investigations on the plankton community of Balsfjorden, Northern Norway. *Sarsia*, **69**, 1–15.

Erga, S. R. (1989) Ecological studies on the phytoplankton of Boknafjorden, Western Norway. 1. The effect of water exchange processes and environmental factors on temporal and vertical variability of biomass. *Sarsia*, **74**, 161–176.

Fouilland, E., Reymond, J. G., Leakey, J. G. *et al.* (2007) The response of a planktonic microbial community to experimental simulations of sudden mixing conditions in temperate coastal waters: importance of light regime and nutrient enrichment. *J. Exp. Mar. Biol. Ecol.*, **351**, 211–225.

Gaard, E., Gislason, A. and Melle, W. (2006) Iceland, Faroe and Norwegian coasts. In Robinson, A. R. and Brink, K. H. (eds), *The Sea. The Global Coastal Ocean. Interdisciplinary Regional Studies and Syntheses: President and Fellowship of Harvard University*, Vol. 14, Part B., pp. 1077–1109.

Gillibrand, P. A., Cage, A. G. and Austin, W. E. N. (2005) A preliminary investigation of basin water response to climate forcing in a Scottish fjord: evaluating the influence of the NAO. *Cont. Shelf Res.*, **25**, 571–587.

Grasshoff, K., Erhardt, M. and Kremling, K. (eds.) (1999) *Methods for Seawater Analysis*, 3rd edn. Wiley-Weinheim, 600 pages.

Gudmundsson, K. (2002) Chlorophyll and phytoplankton growth in Mjodifjordur. In: Gunnarson, K, editor. Environment, phytoplankton, and mussels in Mjodifjordur. *Mar. Res. Inst. Rep. Ser.*, **92**, 57–68.

Hansen, B., Eliasen, S. K., Gaard, E. *et al.* (2005) Climatic effects on plankton and productivity on the Faroe Shelf. *ICES J. Mar. Sci.*, **62**, 1224–1232.

Jeffrey, S. W. and Humphrey, G. F. (1975) New spectrophotometric equations for determining chlorophylls *a*, *b*, c_1 and c_2 in higher plants, algae and natural phytoplankton. *Biochem. Physiol. Pflanz.*, **167**, 191–194.

Jespersen, A. M. (1994) Comparison of $^{14}CO_2$ uptake and release rates in laboratory cultures of phytoplankton. *Oikos*, **69**, 460–468.

Jones, K. J. and Gowen, R. J. (1990) Influence of stratification and irradiance regime on summer phytoplankton composition in coastal and shelf seas in the British Isles. *Estuar. Coast. Shelf Sci.*, **30**, 557–567.

Kiørboe, T. (1993) Turbulence, phytoplankton cell size, and the structure of pelagic food webs. *Adv. Mar. Biol.*, **29**, 1–72.

Knudsen, M. (1900) Ein hydrographische Lehrsatz. *Ann. Hydrogr. Mar. Met.*, **28**, 316–320.

Langdon, C. (1988) On the causes of interspecific differences in growth-irradiance relationship for phytoplankton. II. A general review. *J. Plankton Res.*, **10**, 1291–1312.

Mann, K. H. (2000) *Ecology of Coastal Waters. With Implications for Management*, 2nd edn, Blackwell Science, Massachusetts, USA, 406 pages.

Mann, K. H. and Lazier, J. R. N. (2006) *Dynamics of Marine Ecosystems. Biological–Physical Interactions in the Oceans*, 3rd edn: Blackwell Science, MA, USA, 496 pages.

Margalef, R. (1978) Life forms of phytoplankton as survival alternatives in an unstable environment. *Ocean. Acta.*, **1**, 493–509.

Marra, J. (2002) Approaches to the measurements of plankton production, Chapter 4. In Williams, P. J. le B., Thomas, D. N. and Reynolds, C. S. (eds), *Plankton Productivity*. Blackwell Science, Oxford, UK. pp. 78–108.

Marra, J. (2004) The compensation irradiance for phytoplankton in nature. *Geophys. Res. Lett.*, **31**, L06305. doi:10.1029/2003GL018881.

Mortensen, K. (1990) Sources to nitrogen, phosphor, and organic matter in Skalafjord, Sundalagið and Kaldbaksfjord. *Fiskirannsóknir*, **6**, 287–309 (in Faroese with English summary).

Nelson, D. M. and Smith, W. O. Jr. (1991) Sverdrup revisited critical depths, maximum chlorophyll levels, and the control of Southern Ocean productivity by the irradiance-mixing regime. *Limnol. Oceanogr.*, **36**, 1650–1661.

Parsons, T. R. Y., Maita, Y. and Lalli, C. M. (1984) *A Manual of Chemical and Biological Methods for Seawater Analysis*. Pergamon Press, Oxford, UK, 173 pages.

Rees, A. P., Owens, N. J. P., Heath, M. R. *et al.* (1995) Seasonal nitrogen assimilation and carbon fixation in a fjordic sea loch. *J. Plankton Res.*, **17**, 1307–1324.

Rousseau, V., Leynaert, A., Daoud, N. *et al.* (2002) Diatom succession, silicification and silicic acid availability in Belgian coastal waters (southern North Sea). *Mar. Ecol. Prog. Ser.*, **236**, 61–73.

Sakshaug, E., Kristiansen, S. and Syvertsen, E. (1992) Planktonalger. Chapter 6. In Sakshaug, E., Bjørke, A., Gulliksen, B. *et al.* (eds), *Økosystem Barentshavet [The Barent Sea Ecosystem]*, Pro Mare. Trondheim. pp. 79–108.

Smyth, T. J., Pemberton, K. L., Aitken, J. *et al.* (2004) A methodology to determine primary production and phytoplankton photosynthetic parameters from Fast Repetition Rate Fluorometry. *J. Plankton Res.*, **26**, 1337–1350.

Steingrund, P., Hansen, B. and Gaard, E. (2005) Cod in Faroese Waters. Spawning and life history information for North Atlantic cod stocks. *ICES Cooperative Res. Rep.*, **274**, 50–55.

Suggett, D. J., Moore, C. M., Hickman, A. E. *et al.* (2009) Interpretation of fast repetition rate (FRR) fluorescence: signatures of phytoplankton community versus physiological state. *Mar. Ecol. Prog. Ser.* **376**, 1–19.

Sverdrup, H. U. (1953) On conditions for the vernal blooming of phytoplankton. *J. Conseil. Cons. Perm. Int. pour ÍExpl. Mer*, **18**, 287–295.

Thordardottir, T. (1976) Preliminary assessment of the annual production in the shelf area around Iceland. *ICES CM* 1976/L:32, 4 pp.

Wassmann, P. (1990) Relationship between primary and export production in the boreal coastal zone of the North Atlantic. *Limnol. Oceanogr.*, **35**, 464–471.